Accepted for publication in ApJ Letters
Preprint typeset using LATEX style emulateapj

THE ORIGIN OF DIVERSITY OF TYPE IA SUPERNOVAE AND ENVIRONMENTAL EFFECTS

Hideyuki Umeda, Ken'ichi Nomoto, Chiaki Kobayashi
Department of Astronomy and Research Center for the Early Universe, University of Tokyo, Bunkyo-ku, Tokyo 113-0033, Japan
e-mail: umeda@astron.s.u-tokyo.ac.jp, nomoto@astron.s.u-tokyo.ac.jp, chiaki@astron.s.u-tokyo.ac.jp
Izumi Hachisu
Department of Earth Science and Astronomy, College of Arts and Sciences, University of Tokyo, Meguro-ku, Tokyo 153-8902, Japan
e-mail: hachisu@chianti.c.u-tokyo.ac.jp
Mariko Kato
Department of Astronomy, Keio University, Hiyoshi, Kouhoku-ku, Yokohama 223-8521, Japan
e-mail: mariko@educ.cc.keio.ac.jp

ABSTRACT

Observations suggest that the properties of Type Ia supernovae (SNe Ia) may depend on environmental characteristics, such as morphology, metallicity, and age of host galaxies. The influence of these environmental properties on the resulting SNe Ia is studied in this paper. First it is shown that the carbon mass fraction X(C) in the C+O white dwarf SN Ia progenitors tends to be smaller for lower metallicity and older the binary system age. It is then suggested that the variation of X(C) causes the diversity in the brightness of SNe Ia: a smaller X(C) leads to a dimmer SN Ia. Further studies of the propagation of the turbulent flame are necessary to confirm this relation. Our model for the SN Ia progenitors then predicts that when the progenitors belong to an older population or to a low metallicity environment, the number of bright SNe Ia is reduced, so that the variation in brightness among the SNe Ia is also smaller. Thus our model can explain why the mean SN Ia brightness and its dispersion depend on the morphology of the host galaxies and on the distance of the SN from the center of the galaxy. It is further predicted that at higher redshift ($z \gtrsim 1$) both the the mean brightness of SNe Ia and its variation should be smaller in spiral galaxies than in elliptical galaxies. These variations are within the range observed in nearby SNe Ia. In so far as the variation in X(C) is the most important cause for the diversity among SNe Ia, the light curve shape method currently used to determine the absolute magnitude of SNe Ia can be applied also to high redshift SNe Ia.

Subject headings: stars: white dwarfs — stars: evolution — binaries: close — supernovae: general — cosmology: miscellaneous

1. INTRODUCTION

It is widely accepted that Type Ia supernovae (SNe Ia) are thermonuclear explosions of accreting C+O white dwarfs (WDs), although the nature of the progenitor binary system and the detail of the explosion mechanism are still under debate.

SNe Ia are good distance indicators, and provide a promising tool for determining cosmological parameters (e.g., Branch and Tammann 1992). From the observations of high redshift SNe Ia, both the SN Cosmology Project (Perlmutter et al. 1999) and the High-z SN Search Team (Riess et al. 1998) have suggested a statistically significant value for the cosmological constant. However, SNe Ia are not perfect standard candles, but show some intrinsic variations in brightness. When determining the absolute peak luminosity of high-redshift SNe Ia, therefore, these analyses have taken advantage of the empirical relation existing between the peak brightness and the light curve shape (LCS). Since this relation has been obtained from nearby SNe Ia only (Phillips 1993; Hamuy et al. 1995; Riess, Press & Kirshner 1995), it is important to examine whether it depends systematically on environmental properties such as metallicity and age of the progenitor system. This *Letter* addresses the issue of whether a difference in the environmental properties is at the basis of the observed range of peak brightness.

There are some observational indications that SNe Ia are affected by their environment. The most luminous SNe Ia seem to occur only in spiral galaxies, while both spiral and elliptical galaxies are hosts for dimmer SNe Ia. Thus the mean peak brightness is dimmer in ellipticals than in spiral galaxies (Hamuy et al. 1996). The SNe Ia rate per unit luminosity at the present epoch is almost twice as high in spirals as in ellipticals (Cappellaro et al. 1997). Moreover, Wang, Höflich & Wheeler (1997) and Riess et al. (1999) found that the variation of the peak brightness for SNe located in the outer regions in galaxies is smaller.

Höflich, Wheeler, & Thielemann (1998) examined how the initial composition of the WD (metallicity and the C/O ratio) affects the observed properties of SNe Ia. Umeda et al. (1999) obtained the C/O ratio as a function of the main-sequence mass and metallicity of the WD progenitors. In this *Letter* we suggest that the variation of the C/O ratio is the main cause of the variation of SNe Ia brightness, with larger C/O ratio yielding brighter SNe Ia (§ 2). We then show that the C/O ratio depends indeed on environmental properties, such as the metallicity and age of the companion of the WD (§ 3), and that our model can explain most of the observational trends discussed above (§4). We then make some predictions about the brightness of SN Ia at higher redshift (§5).

2. EXPLOSION MODEL AND THE C/O RATIO OF WD PROGENITORS

For the progenitors of SNe Ia, we adopt the single degenerate (SD) Chandrasekhar mass model, in which an accreting C-O WD explodes when its mass reaches the critical mass $M_{\rm Ia} \simeq 1.37 - 1.38 M_\odot$ (Nomoto, Thielemann, & Yokoi 1984). Merging of white dwarfs is likely to lead to accretion-induced-collapse rather than thermonuclear explosion (Saio & Nomoto 1998). Chandrasekhar mass models can reproduce well the spectrum and the light curves of SNe Ia, assuming either the explosion is induced by a deflagration or by a delayed detonation (Höflich & Khokhlov 1996; Nugent et al. 1997). In these models, the brightness of SNe Ia is determined mainly by the mass of ^{56}Ni synthesized ($M_{\rm Ni56}$). Observational data suggest that $M_{\rm Ni56}$ for most SNe Ia lies in the range $M_{\rm Ni56} \sim 0.4 - 0.8 M_\odot$ (e.g. Mazzali et al. 1998). This range of $M_{\rm Ni56}$ can result from differences in the C/O ratio in the progenitor WD as follows.

In the deflagration model, a faster propagation of the convective deflagration wave results in a larger $M_{\rm Ni56}$. For example, a variation of the propagation speed by 15% in the W6 – W8 models results in $M_{\rm Ni56}$ values ranging between 0.5 and $0.7 M_\odot$ (Nomoto et al. 1984), which could explain the observations. The actual propagation of the deflagration depends on the highly non-linear behavior of the turbulent flame (Niemeyer & Hillebrand 1995), and so it may be very sensitive to the C/O ratio. Qualitatively, a larger C/O ratio leads to the production of more nuclear energy and buoyancy force, thus leading to a faster propagation and a larger $M_{\rm Ni56}$. Quantitatively, further studies of the turbulent flame are necessary to confirm that the expected range of C/O results in the required 15-20% variation of the flame speed.

In the delayed detonation model, $M_{\rm Ni56}$ is predominantly determined by the deflagration-to-detonation-transition (DDT) density $\rho_{\rm DDT}$, at which the initially subsonic deflagration turns into a supersonic detonation (Khokhlov 1991). We reproduce the relation between $\rho_{\rm DDT}$ and $M_{\rm Ni56}$ in Figure 1 by performing hydrodynamical calculations for several values of $\rho_{\rm DDT}$, as in Nomoto et al. (1997), Kishimoto et al. (1999), and Iwamoto et al. (1999). The pre-explosive WD model is model C6 (Nomoto et al. 1984), and the flame speed of the initial deflagration is assumed to be 3% of the local sound velocity. Figure 1 shows that if the transition density varies in the range $\rho_{\rm DDT} \simeq 1.3 - 3 \times 10^7$ g cm^{-3}, the resulting variation of $M_{\rm Ni56}$ is large enough to explain the observations.

Possible mechanisms for DDT to occur have been studied by Arnett & Livne (1994), Niemeyer & Woosley (1997), and Khokhlov, Oran & Wheeler (1997): when the deflagration wave reaches a sufficiently low density, $\rho \sim 10^7$ g cm^{-3}, the turbulent motion associated with the flame may destroy the burning front. The resulting turbulent mixing between ashes and fuels efficiently heats up the fuel and could produce a region with a very shallow temperature gradient. In such a region, successive spontaneous ignitions cause the over-driven deflagration to propagate supersonically. This may induce a detonation wave if the mass of the region exceeds a critical mass $\Delta M_{\rm DDT}$. This critical mass is quite sensitive to the carbon mass fraction X(C), e.g. $\Delta M_{\rm DDT} \sim 10^{-19}$ and $10^{-14} M_\odot$ at $\rho = 3 \times 10^7$ g cm^{-3} for X(C) = 1.0 and 0.5, respectively (Niemeyer & Woosley 1997). Though the exact value of $\rho_{\rm DDT}$ is still debated, and its dependence on X(C) has not been studied, it is not unlikely that for a larger X(C) DDT can occur at larger $\rho_{\rm DDT}$. Hence a larger X(C) is likely to result in a larger $\rho_{\rm DDT}$ and $M_{\rm Ni56}$.

In this *Letter*, therefore, we postulate that $M_{\rm Ni56}$ and consequently brightness of a SN Ia increase as the progenitors' C/O ratio increases, as illustrated in Figure 1, where the range of $M_{\rm Ni56} \sim 0.5 - 0.8 M_\odot$ is the result of an X(C) range $0.35 - 0.5$, which is the range of X(C) values of our progenitor models described below (Figure 2). The X(C) – $M_{\rm Ni56}$ relation we adopt is still only a working hypothesis, which needs to be proved from studies of the turbulent flame during explosion.

Höflich et al. (1998) considered the dependence on X(C) but they assumed in their DDT model that $\rho_{\rm DDT}$ and X(C) are independent parameters. They showed that for the same $\rho_{\rm DDT}$ a smaller X(C) leads to a slightly brighter SN Ia despite a slightly smaller $M_{\rm Ni56}$ produced, because a smaller fraction of the explosion energy goes into the kinetic energy. In this *Letter* we assume that X(C) is the primary parameter to determine $\rho_{\rm DDT}$ and thus $M_{\rm Ni56}$. The assumed variation of $M_{\rm Ni56}$ is so large that a smaller X(C) yields an intrinsically dimmer SN.

3. METALLICITY AND AGE EFFECTS

In this section we discuss how the C/O ratio in the WD depends on the metallicity and age of the binary system. The C/O ratio in C+O WDs depends primarily on the main-sequence mass of the WD progenitor and on metallicity. According to the evolutionary calculations for 3−9 $M_\odot$ stars by Umeda et al. (1999), the C/O ratio and its distribution are determined in the following evolutionary stages of the close binary.

1) At the end of central He burning in the 3−9 $M_\odot$ primary star, C/O$<$ 1 in the convective core. The mass of the core is larger for more massive stars. 2) After central He exhaustion, the outer C+O layer grows via He shell burning, where C/O$\gtrsim$ 1 (Umeda et al. 1999). 3a) If the primary star becomes a red giant (case C evolution; e.g. van den Heuvel 1994), it then undergoes the second dredge-up, forming a thin He layer, and enters the AGB phase. The C+O core mass, $M_{\rm CO}$, at this phase is larger for more massive stars. For a larger $M_{\rm CO}$ the total carbon mass fraction is smaller. 4a) When it enters the AGB phase, the star greatly expands and is assumed here to undergo Roche lobe overflow (or a super-wind phase) and to form a C+O WD. Thus the initial mass of the WD, $M_{\rm WD}^{(0)}$, in the close binary at the beginning of mass accretion is approximately equal to $M_{\rm CO}$. 3b) If the primary star becomes a He star (case BB evolution), the second dredge-up in (3a) corresponds to the expansion of the He envelope. 4b) The ensuing Roche lobe overflow again leads to a white dwarf of mass $M_{\rm WD}^{(0)} = M_{\rm CO}$.

5) After the onset of mass accretion, the WD mass grows through steady H burning and weak He shell flashes, as described in the WD wind model (Hachisu, Kato, & Nomoto 1996, 1999, and Hachisu et al. 1999; hereafter, HKN96, HKN99, and HKNU99, respectively). The composition of the growing C+O layer is assumed to be C/O=1. 6)

The WD grows in mass and ignites carbon when its mass reaches $M_{\rm Ia} = 1.367 M_\odot$, as in the model C6 of Nomoto et al. (1984). Because of strong electron-degeneracy, carbon burning is unstable and grows into a deflagration for a central temperature of 8×10^8 K and a central density of 1.47×10^9 g cm^{-3}. At this stage, the convective core extends to $M_r = 1.14 M_\odot$ and the material is mixed almost uniformly, as in the C6 model.

In Figure 2 we show the carbon mass fraction X(C) in the convective core of this pre-explosive WD, as a function of metallicity (Z) and initial mass of the WD before the onset of mass accretion, $M_{\rm CO}$. Figure 2 reveals that: 1) X(C) is smaller for larger $M_{\rm CO}$. 2) The dependence of X(C) on metallicity is small when plotted against $M_{\rm CO}$, even though the relation between $M_{\rm CO}$ and the initial stellar mass depends sensitively on Z (Umeda et al. 1999).

Metallicity dependent wind during mass accretion: In the SD Chandrasekhar mass model for SNe Ia, a WD explodes as a SN Ia only when its rate of the mass accretion ($\dot{M}$) is in a certain narrow range (e.g., Nomoto & Kondo 1991). HKN96 showed that the accreting WD blows a strong wind if $\dot{M}$ exceeds the rate $\dot{M}_{\rm b}$ at which steady burning can process the accreted hydrogen into He. If the wind is sufficiently *strong* (i.e., the wind velocity $v_{\rm w}$ exceeds the escape velocity $v_{\rm esc}$ of the WD), the WD can avoid the formation of a common envelope and increase its mass continuously at a rate $\dot{M}_{\rm b}$ by blowing the extra mass away in a wind.

In this model, which is adopted in the present study, an interesting metallicity effect has been found (Kobayashi et al. 1998; Hachisu & Kato 1999). The wind velocity is higher for larger $M_{\rm WD}$ and larger Fe/H because of higher luminosity and larger opacity, respectively. In order to blow sufficiently strong wind (i.e., $v_{\rm w} > v_{\rm esc}$), $M_{\rm WD}$ should exceed a certain mass $M_{\rm w}$ (Fig. 6 of HKN99). As seen in Figure 1 of Kobayashi et al. (1998), $M_{\rm w}$ is larger for lower metallicity; e.g., $M_{\rm w} = 0.65$, 0.85, and 0.95 $M_\odot$ for $Z = 0.02$, 0.01, and 0.004, respectively. In order for a WD to grow its mass at $\dot{M} > \dot{M}_{\rm b}$, its initial mass $M_{\rm CO}$ should exceed $M_{\rm w}$. In other words, $M_{\rm w}$ is the metallicity-dependent minimum $M_{\rm CO}$ required for a WD to become an SN Ia (*strong wind condition* in Fig.2). The upper bound $M_{\rm CO} \simeq 1.07 M_\odot$ is imposed by the condition that carbon should not ignite and is almost independent of metallicity.

As shown in Figure 2, the range of $M_{\rm CO}$ can be converted into a range of X(C). From this we find the following metallicity dependence for X(C): 1) The upper bound of X(C), which is determined by the lower limit on $M_{\rm CO}$ imposed by the metallicity-dependent conditions for a strong wind, e.g., $X({\rm C}) \lesssim 0.51$, 0.46 and 0.41, for Z=0.02, 0.01, and 0.004, respectively. 2) On the other hand, the lower bound, $X({\rm C}) \simeq 0.35 - 0.33$, does not depend much on Z, since it is imposed by the maximum $M_{\rm CO}$. 3) Assuming the relation between $M_{\rm Ni56}$ and X(C) given in Figures 1 and 2, our model predicts the absence of brighter SNe Ia in lower metallicity environment.

Age effects: In our model, the age of the progenitor system also constrains the range of X(C) in SNe Ia. In the SD scenario, the lifetime of the binary system is essentially the main-sequence lifetime of the companion star, which depends on its initial mass M_2. HKNU99 and HKN99 have obtained a constraint on M_2 by calculating the evolution of accreting WDs for a set of initial masses of the WD ($M_{\rm WD}^{(0)} \simeq M_{\rm CO}$) and of the companion ($M_2$), and the initial binary period (P_0). In order for the WD mass to reach $M_{\rm Ia}$, the donor star should transfer enough material at the appropriate accretion rates. The donors of successful cases are divided into two categories: one is composed of slightly evolved main-sequence stars with $M_2 \sim 1.7 - 3.6 M_\odot$ (for Z=0.02), and the other of red-giant stars with $M_2 \sim 0.8 - 3.1 M_\odot$ (for Z=0.02) (HKN99, HKNU99; also Li & van den Heuvel 1997).

If the progenitor system is older than 2 Gyr, it should be a system with a donor star of $M_2 < 1.7 M_\odot$ in the red-giant branch. Systems with $M_2 > 1.7 M_\odot$ become SNe Ia in a time shorter than 2 Gyr. Likewise, for a given age of the system, M_2 must be smaller than a limiting mass. This constraint on M_2 can be translated into the presence of a minimum $M_{\rm CO}$ for a given age, as follows: For a smaller M_2, i.e. for the older system, the total mass which can be transferred from the donor to the WD is smaller. In order for $M_{\rm WD}$ to reach $M_{\rm Ia}$, therefore, the initial mass of the WD, $M_{\rm WD}^{(0)} \simeq M_{\rm CO}$, should be larger. This implies that the older system should have larger minimum $M_{\rm CO}$ as indicated in Figure 2. Using the $X({\rm C}) - M_{\rm CO}$ and $M_{\rm Ni56} - {\rm X}(C)$ relations (Figs. 1 and 2), we conclude that WDs in older progenitor systems have a smaller X(C), and thus produce dimmer SNe Ia.

4. COMPARISON WITH OBSERVATIONS

The first observational indication which can be compared with our model is the possible dependence of the SN brightness on the morphology of the host galaxies. Hamuy et al. (1996) found that the most luminous SNe Ia occur in spiral galaxies, while both spiral and elliptical galaxies are hosts to dimmer SNe Ia. Hence, the mean peak brightness is lower in elliptical than in spiral galaxies.

In our model, this property is simply understood as the effect of the different age of the companion. In spiral galaxies, star formation occurs continuously up to the present time. Hence, both WD+MS and WD+RG systems can produce SNe Ia. In elliptical galaxies, on the other hand, star formation has long ended, typically more than 10 Gyr ago. Hence, WD+MS systems can no longer produce SNe Ia. In Figure 3 we show the frequency of the expected SN I for a galaxy of mass $2 \times 10^{11} M_\odot$ for WD+MS and WD+RG systems separately as a function of $M_{\rm CO}$. Here we use the results of HKN99 and HKNU99, and the $M_{\rm CO} - X({\rm C})$ and $M_{\rm Ni56} - X({\rm C})$ relations given in Figure 2. Since a WD with smaller $M_{\rm CO}$ is assumed to produce a brighter SN Ia (larger $M_{\rm Ni56}$), our model predicts that dimmer SNe Ia occur both in spirals and in ellipticals, while brighter ones occur only in spirals. The mean brightness is smaller for ellipticals and the total SN Ia rate per unit luminosity is larger in spirals than in ellipticals. These properties are consistent with observations.

The second observational suggestion is the radial distribution of SNe Ia in galaxies. Wang et al. (1997) and Riess et al. (1998) found that the variation of the peak brightness for SNe Ia located in the outer regions in galaxies is smaller. This behavior can be understood as the effect of metallicity. As shown in Figure 2, even when the progenitor age is the same, the minimum $M_{\rm CO}$ is larger for a smaller metallicity because of the metallicity dependence of the WD winds. Therefore, our model predicts that the maximum brightness of SNe Ia decreases as metallicity decreases. Since the outer regions of galaxies are thought to have lower metallicities than the inner regions (Zaritsky, Kennicutt, Huchra 1994; Kobayashi & Arimoto 1999), our model is consistent with observations. Wang et al. (1997) also claimed that SNe Ia may be deficient in the bulges of spiral galaxies. This can be explained by the age effect, because the bulge consists of old population stars.

5. CONCLUSIONS AND DISCUSSION

We have suggested that $X(\mathrm{C})$ is the quantity very likely to cause the diversity in M_{Ni56} and thus in the brightness of SNe Ia. We have then shown that our model predicts that the brightness of SNe Ia depends on the environment, in a way which is qualitatively consistent with the observations. Further studies of the propagation of the turbulent flame and the DDT are necessary in order to actually prove that $X(\mathrm{C})$ is the key parameter.

Our model predicts that when the progenitors belong to an old population, or to a low metal environment, the number of very bright SNe Ia is small, so that the variation in brightness is also smaller. In spiral galaxies, the metallicity is significantly smaller at redshifts $z \gtrsim 1$, and thus both the mean brightness of SNe Ia and its range tend to be smaller. At $z \gtrsim 2$ SNe Ia would not occur in spirals at all because the metallicity is too low. In elliptical galaxies, on the other hand, the metallicity at redshifts $z \sim 1-3$ is not very different from the present value. However, the age of the galaxies at $z \simeq 1$ is only about 5 Gyr, so that the mean brightness of SNe Ia and its range tend to be larger at $z \gtrsim 1$ than in the present ellipticals because of the age effect.

We note that the variation of $X(\mathrm{C})$ is larger in metal-rich nearby spirals than in high redshift galaxies. Therefore, if $X(\mathrm{C})$ is the main parameter responsible for the diversity of SNe Ia, and if the LCS method is confirmed by the nearby SNe Ia data, the LCS method can also be used to determine the absolute magnitude of high redshift SNe Ia.

We wish to thank P. Mazzali, K. Iwamoto and N. Kishimoto for useful discussion and suggestions. This work has been supported in part by the grant-in-Aid for Scientific Research (0980203, 09640325) and COE research (07CE2002) of the Ministry of Education, Science, Culture and Sports in Japan.

REFERENCES

Arnett, W.D. & Livne, E. 1994, ApJ, 427, 314
Branch, D., & Tammann, G.A. 1992, ARA&A, 30, 359
Capellaro, E., Turatto, M., Tsvetkov, D.Yu., Bartunov, O.S., Pollas, C., Evans, R., & Hamuy, M. 1997 A&A, 322, 431
Hachisu, I., Kato, M., & Nomoto, K. 1996, ApJ, 470, L97 (HKN96)
Hachisu, I., Kato, M., & Nomoto, K. 1999, ApJ, 521, in press (astro-ph/9902304; HKN99)
Hachisu, I., Kato, M., Nomoto, K., & Umeda, H. 1999, ApJ, 519, in press (astro-ph/9902303; HKNU99)
Hachisu, I. & Kato, M. 1999, in preparation
Hamuy, M., et al. 1995, AJ, 109, 1
Hamuy, M., Phillips, M.M., Schommer, R.A., & Suntzeff, N.B. 1996, AJ, 112, 2391
Höflich, P., & Khokhlov, A. 1996, ApJ, 457, 500
Höflich, P., Wheeler, J.C., & Thielemann, F.-K. 1998, ApJ, 495, 617
Iwamoto, K., Brachwitz, F., Nomoto, K., Kishimoto, N., Umeda, H., Hix, W. R., Thielemann, F-K. 1999, ApJ, submitted
Khokhlov, A. 1991, A&A, 245, 114
Khokhlov, A.M., Oran, E.S., & Wheeler, J.C. 1997, ApJ, 478, 678
Kishimoto, N., Iwamoto, K., Umeda, H., Nomoto, K., Brachwitz, F., Hix, W. R., & Thielemann, F-K., 1999, in Origin of Matter and Evolution of Galaxies 97, eds. S. Kubono et al. (Singapore: World Scientific), 378
Kobayashi, C., & Arimoto, N. 1998, ApJ, submitted
Kobayashi, C., Tsujimoto, T., Nomoto, K., Hachisu, I., & Kato, M. 1998, ApJ, 503, L155
Li, X.-D., & van den Heuvel, E. P. J. 1997, A&A, 322, L9
Mazzali, P. A., Cappellaro, E., Danziger, I. J., Turatto, M., & Benetti, S. 1998, ApJ, 499, L49
Niemeyer J.C., & Hillebrandt W. 1995, ApJ, 452, 769
Niemeyer, J.C., & Woosley, S.E. 1997, ApJ, 475, 740
Nomoto, K., Thielemann, F. -K., & Yokoi, K. 1984, ApJ, 286, 644
Nomoto, K., & Kondo, Y. 1991, ApJ, 367, l19
Nomoto, K., et al. 1997, in Thermonuclear Supernovae, Eds. P.Ruiz-Lapuente et al. (Dordrecht: Kluwer), 349
Nugent, P., Baron, E., Branch, D., Fisher, A., & Hauschildt, P.H. 1997, ApJ, 485, 812
Perlmutter, S. et al. 1999, ApJ, in press, astro-ph/9812133
Phillips, M. M. 1993, ApJ, 413, L75
Riess, A.G., Press, W.H., & Kirshner, R.P. 1995, ApJ, 438, L17
Riess, A.G. et al. 1998, AJ, 116, 1009
Riess, A. G. et al. 1999, AJ, 117, 707
Saio, H., & Nomoto, K. 1998, ApJ, 500, 388
Umeda, H., Nomoto, K., Yamaoka, H., & Wanajo, S. 1999, ApJ, 513, 861
van den Heuvel, E.P.J., 1994, in Interacting Binaries, eds. S.N. Shore et al. (Berlin: Springer-Verlag), 263
Wang, L., Höflich, P., & Wheeler, J. C. 1997, ApJ, 483, L29
Zaritsky, D., Kennicutt, R.C., & Huchra, J.P. 1994, ApJ, 420, 87

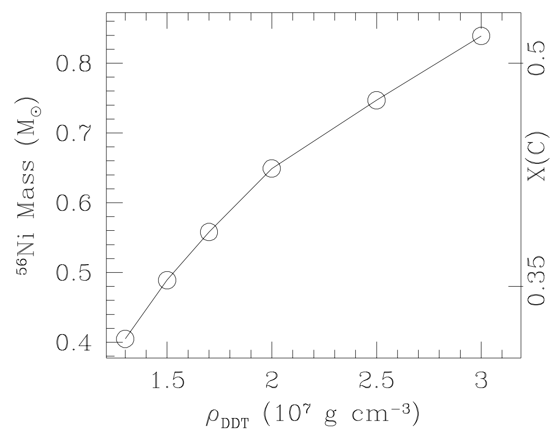

FIG. 1.— Deflagration to detonation transition density ($\rho_{\rm DDT}$) vs. ^{56}Ni mass ($M_{\rm Ni56}$). The X(C) axis is approximately given as discussed in § 2. These results are obtained for X(C)=0.43. For a given $\rho_{\rm DDT}$ varying X(C) between X(C)=0.35 − 0.50 changes the ^{56}Ni mass only by $\sim \pm 0.02 M_\odot$.

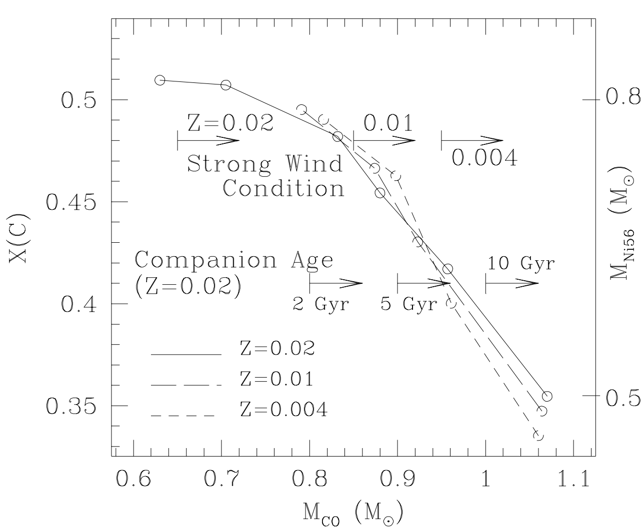

FIG. 2.— The total ^{12}C mass fraction included in the convective core of mass, $M = 1.14 M_\odot$, just before the SN Ia explosion as a function of the C+O core mass before the onset of mass accretion, $M_{\rm CO}$. The lower bounds of $M_{\rm CO}$ obtained from the age effects and the conditions for strong wind to blow are also shown by arrows. The axis of $M_{\rm Ni56}$ is obtained from the X(C) $- M_{\rm Ni56}$ relation assumed in Figure 1.

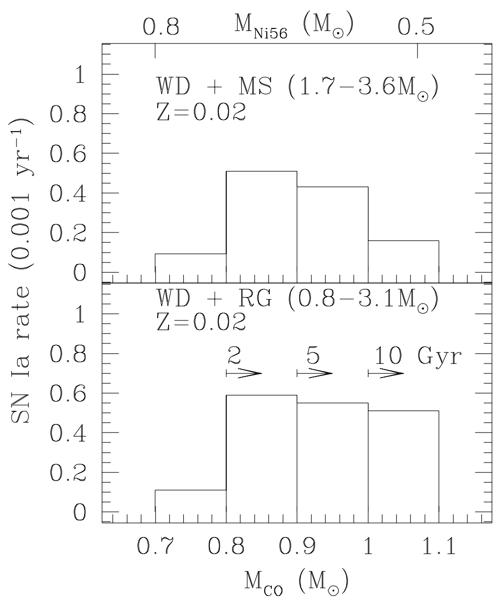

Fig. 3.— SN Ia frequency for a galaxy of mass $2 \times 10^{11} M_{\odot}$ as a function of $M_{\rm CO}$ for Z=0.02. For the WD+RG system, constraints from the companion's age are shown by the arrows. SNe Ia from the WD+MS system occur in spirals but not in ellipticals because of the age effect. $M_{\rm CO}$ and $M_{\rm Ni56}$ can be related as shown here if the $X(\rm C) - M_{\rm Ni56}$ relation in Figure 1 is adopted.